Q^2 Measurement for PREX

Nilanga K. Liyanage, Kiadtisak Saenboonruang
University of Virginia

Robert Michaels
Thomas Jefferson National Accelerator Facility

July 18, 2011

This report discusses the Q^2 measurement for PREX run during March-June 2010 (Table 1). This report also discusses the systematic errors due to beam energy, final momentum of scattered electrons, scattering angle, pileup, and trigger bias. For PREX, uncertainty from scattering angle measurement is the main contribution to the systematic error in Q^2.

Beam Energy (GeV)	1.0605
LHRS θ_0 ($^\circ$)	5.0649
RHRS θ_0 ($^\circ$)	4.9332
Average LHRS Q^2 (GeV^2)	0.009330
Average RHRS Q^2 (GeV^2)	0.008751
Average Q^2 (GeV^2)	0.009066

Table 1: Q^2 and useful information for PREX

Contents

List of Figures

List of Tables

1 Q^2 measurement and its components

The four-momentum transfer squared is

$$Q^2 = 2EE'(1 - cos(\theta)) \tag{1}$$

where E is the incident energy, E' is the final momentum of scattered electron and θ is the scattering angle. In the case of elastic electron scattering, one may eliminate one of the three variables and the Q^2 can be written as

1. $Q^2 = 2E^2 f_r(1 - cos(\theta))$
2. $Q^2 = 2E'^2 f'_r(1 - cos(\theta))$
3. $Q^2 = 2m_p(E - E')$

Here f_r and f'_r are recoil factors defined as $f_r = \frac{1}{1+(\frac{E}{m})(1-cos(\theta))}$ and $f'_r = \frac{1}{1-(\frac{E'}{m})(1-cos(\theta))}$. Ideally, these 3 equations would serve as tools for consistency check. However, for PREX, the difference in E and E' was only about 20 keV (after the correction for energy loss before and after scattering) while δE and $\delta E'$ were $\sim$ 200 keV at best. These led to the blow up of δQ^2 in eq.3. Consequently, we could only use eq.1 and eq.2 for consistency check.

In order to accurately measure Q^2, the first component we need is the beam energy. The beam energy was continuously measured to 1×10^{-3} during the run using the Tiefenbach method which had been previously calibrated using two energy measuring apparatus, ARC and eP. Second component needed is the final momentum of scattered electrons. This quantity is well measured to $\sim 5 \times 10^{-4}$ using the high resolution spectrometers (HRS) in Hall A. The last component is the scattering angle. There are two steps involved in measuring the scattering angle:

1. Obtain the spectrometer central angle (θ_0).
2. Obtain the angle of a scattered particles with respect to the spectrometer central angle.

The uncertainty from scattering angle measurement was the main source of the uncertainty in Q^2.

1.1 Beam Energy Measurement

The nominal beam energy for PREX was 1.063 GeV and was continuously measured by the Tiefenbach measurement which had been calibrated using two independent apparatus, ARC and eP. ARC measurement uses the fact that an electron beam would be deflected by a known angle when it passed through a magnetic field. By applying the right magnetic field and fixing angle at 34.3°, one could measure the beam energy precisely. The eP measurement makes use of the fact that, for the elastic $e + p$ reaction, the scattering angles of the electron and proton were related to the energy of the incoming electron. The two measurements are accurate to 3×10^{-4} level. However, since PREX only used the Tiefenbach measurement, beam energy accuracy was limited to $\sim 0.1\%$ level and contributed $\sim 0.1\%$ to systematic error in Q^2.

1.2 Momentum of Scattered Electron Measurement

The final momentum of scattered electrons was measured using the two high resolution spectrometers (HRS) in Hall A. The standard HRS absolute momentum accuracy range of 0.3-4.0 GeV is $\sim 3 \times 10^{-4}$. However,with the installation of a new septum magnet for PREX, the HRS had to be recalibrated. This recalibration was checked using elastic scattering off a thin tantalum target. The momentum accuracy was found to be better than $\sim 0.1\%$ level and contributed $\sim 0.1\%$ to systematic error in Q^2.

1.3 Scattering Angle

Scattering angle is the angle between the direction of a scattered electron and the direction of electron beam. Scattering angle measurement consists of two parts: spectrometer central angle (θ_0) and spectrometer (optics) reconstruction (target angles). Scattering angle (θ) relates to θ_0 and target angles (θ_{tg} and ϕ_{tg}) by

$$\theta = \frac{cos(\theta_0) - \phi_{tg} sin(\theta_0)}{\sqrt{1 + \theta_{tg}^2 + \phi_{tg}^2}} \tag{2}$$

1.3.1 Spectrometer Central Angle

Spectrometer central angle (θ_0) is the angle between spectrometer axis and the ideal beam line. There are two methods to measure θ_0. One way is to perform a *survey*. A survey measures the angle between two imaginary lines: the first line along the ideal spectrometer axis and the second line along the ideal beam line. However, target angles θ_{tg} and ϕ_{tg} are defined with respect to the line from the target center to the central sieve-slit hole. Therefore, translating the central angle from the spectrometer axis to the sieve central line requires surveys of both the target position and the sieve-slit position. The errors from these measurements combined to make the final error of the surveyed angle as much as 0.046° (0.0007 radians). This led to more than 2% uncertainty in Q^2.

A better method to determine θ_0 is to perfrom a *pointing* measurement using differential recoil in elastic scattering. Consider the equation for elastic scattering off a target of mass M_t

$$E' = \frac{(E - E_{loss})}{1 + \frac{2(E-E_{loss})sin^2(\frac{\theta}{2})}{M_t}} - E_{loss} \tag{3}$$

Here, E, E', θ and E_{loss} are beam energy, final momentum, scattering angle and energy loss occurred before and after the scattering respectively. Pointing makes use of the fact that E and M_t are well known. By accurately measuring E', one could precisely calculate θ. The accuracy of this method could be greatly enhanced by considering the difference in E' for elastic scattering off Hydrogen (^{1}H) and some heavier targets.

$E - E'_{Pb}$ (MeV)	1.0
$E - E'_{O}$ (MeV)	1.7
$E - E'_{H}$ (MeV)	5.8

Table 2: $E - E'$ for various nuclei in PREX

For PREX, which ran at a nominal angle of 5°, table 2 gives the values for $E - E'$ for different target used. In this case, θ depended on $E'_2 - E'_H$. Since the energy differences were $\sim$ 5 MeV for PREX, the accuracy of θ measurement depends on how well the spectrometer could measure these

energy differences. This was accomplished by calibrating momentum reconstruction using several targets and different magnetic settings of HRS to sweep the scattered electrons across the entire focal plane. This calibration was checked by measuring the known energy difference between ground state and first excited state of ^{12}C at three different momentum settings.

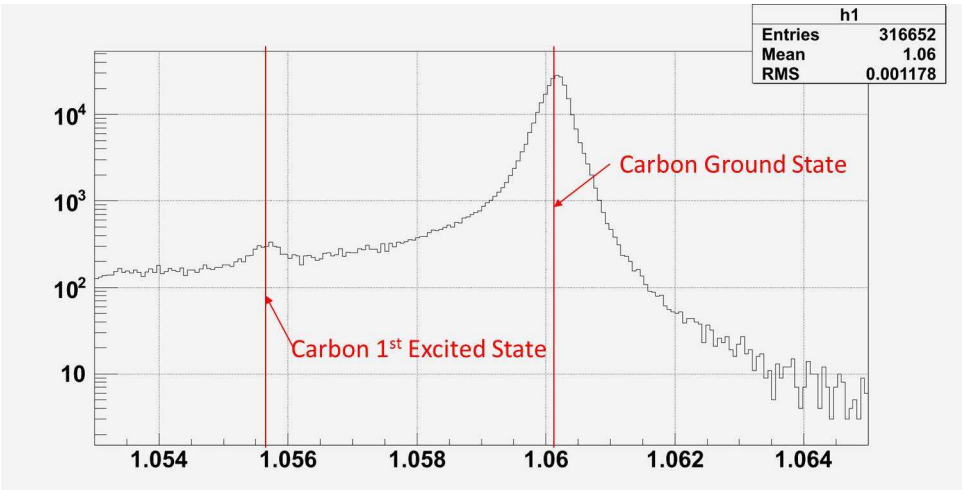

Figure 1: Carbon momentum spectrum after calibration

Run	Momentum Setting (P_0)	$E_0 - E'$ (MeV)
6274	1.063	4.41
6279	1.058	4.50
6289	1.047	4.45

Table 3: $E_0 - E'$ for carbon target on right HRS

Fig. 1 and table 3 shows the difference in energies of ground state and first excited state of ^{12}C (nominal value is 4.44 MeV) after the calibration. The overall accuracy of the momentum reconstruction was 30 keV.

A second major uncertainty could arise due to the energy loss (E_{loss}) in the target. This energy loss was approximately 1 MeV at the center of target. Thus, any uncertainty from E_{loss} estimation could affect the accuracy of

pointing measurement significantly. However, we were able to adequately eliminate this uncertainty by using the difference in E' for two nuclei that are in the same target, where E_{loss} cancels out. The watercell target which consists of ^{16}O and ^{1}H can serve for this purpose. Furthermore, this also eliminated any possible uncertainty due to a beam energy shifted from one run to another. For watercell target, the difference between oxygen and hydrogen elastic peaks is given by:

$$\Delta E' = E'_O - E'_H = E(\frac{1}{1+\frac{2Esin^2(\frac{\theta}{2})}{M_O}} - \frac{1}{1+\frac{2Esin^2(\frac{\theta}{2})}{M_H}}) + correction \qquad (4)$$

where *correction* is the negligible correction term accounted for the differences between M_O and M_H in E_{loss} terms. This term is approximately $\sim 0.1\%$ compared to the main term of $E'_0 - E'_H$.

In order to determine θ_0, we only selected events going through the central sieve-slit hole. We avoided using runs without sieve slit so that the θ_0 measurement does not depend on optics reconstruction. However, they could still be used as a consistency check.

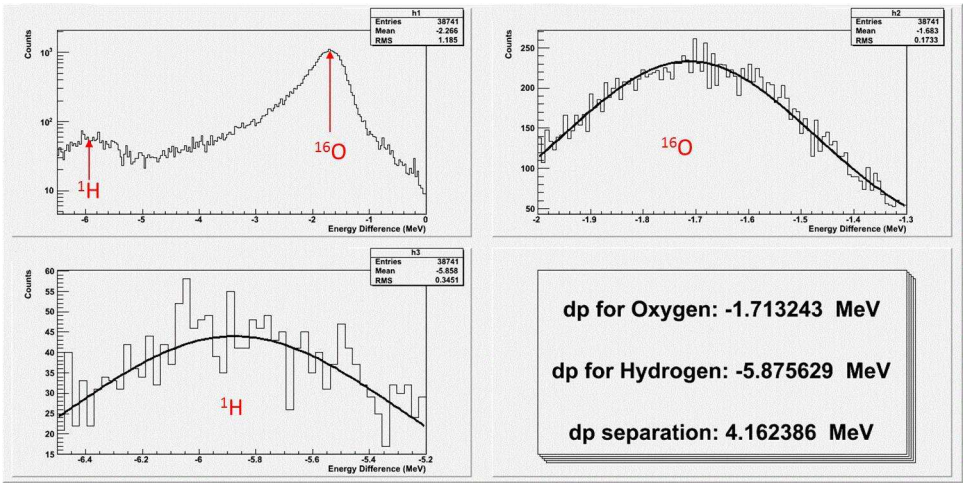

Figure 2: Watercell target momentum spectrum

Run	Momentum Setting (P_0)	$E'_O - E'_H$ (MeV)
26800	1.063	4.24
26822	1.058	4.21
26824	1.047	4.27

Table 4: $E'_0 - E'_H$ for watercell target on left HRS

Run	Momentum Setting (P_0)	$E'_O - E'_H$ (MeV)
6205	1.063	4.09
6233	1.058	4.16
6235	1.047	4.11

Table 5: $E'_0 - E'_H$ for watercell target on right HRS

Pointing measurement was done with three central momentum settings of HRS to increase the accuracy. The oxygen and hydrogen peaks are located in three different areas of the HRS focal plane for the three different momentum settings. Each of the three settings provides an independent measurement of the separation between oxygen and hydrogen peaks. Fig. 2 shows the momentum distribution for watercell target for one of the spectrometer momentum settings. Tables 4 and 5 show the values of $E'_O - E'_H$ for both left and right HRS for the three momentum settings. These values were used to calculate θ_0 by using the least χ^2 method, where χ^2 was defined as $\chi^2 = (\Delta E'_{calc} - \Delta E'_{meas})^2$. $\Delta E'_{calc}$ was calculated using Eq. 3, treating θ as the parameter to be optimized.

Arm	Pointing values (°)	Surveys values (°)
Left	5.065 ± 0.020	5.007 ± 0.046
Right	4.933 ± 0.020	4.910 ± 0.046

Table 6: Spectrometer angles for PREX

The final spectrometer angles determined from this method are given in table 6. Here the spectrometer angle is defined as the angle between the

ideal beamline and the line connecting target center and central sieve-slit hole.

In summary, the accuracy for pointing measurement was 0.020°, while the accuracy for surveys was 0.046°. The pointing measurement improved the angle determination accuracy by two.

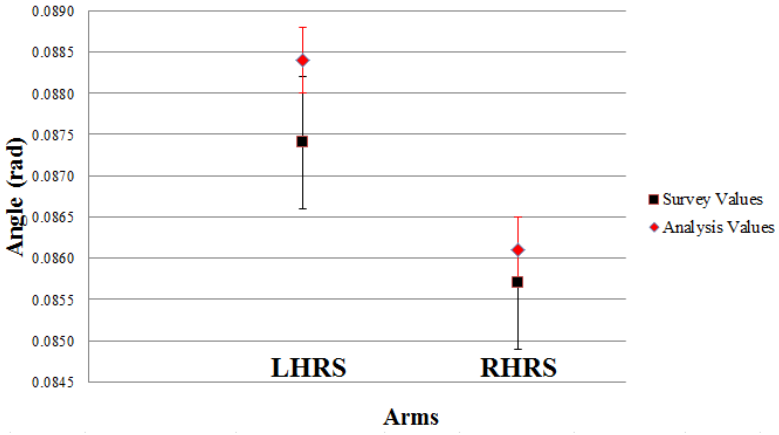

Figure 3: Spectrometer angle (θ_0) comparison between pointing and surveys

1.3.2 Spectrometer (Optics) Reconstruction

Once the pointing measurement has been done, we can obtain the accurate Q^2 at θ_0. However, PREX requires the average Q^2 from the entire acceptance. This requires the optics reconstruction which reconstructed target variables $\delta_{tg}, y_{tg}, \theta_{tg}$ and ϕ_{tg} from focal plane variables $x_{fp}, y_{fp}, \theta_{fp}$ and ϕ_{fp} The reconstruction needed optics database which were well established and tested for standard HRS running but the addition of the new septum magnets created the need for a new database. For this purpose, we used thin carbon, carbon multifoil, tantalum, and watercell targets with sieve slit inserted as a reference for particle tracks. The sieve slit drawing and the optimized left and right θ_{tg} versus ϕ_{tg} sieve patterns are shown in the following figures.

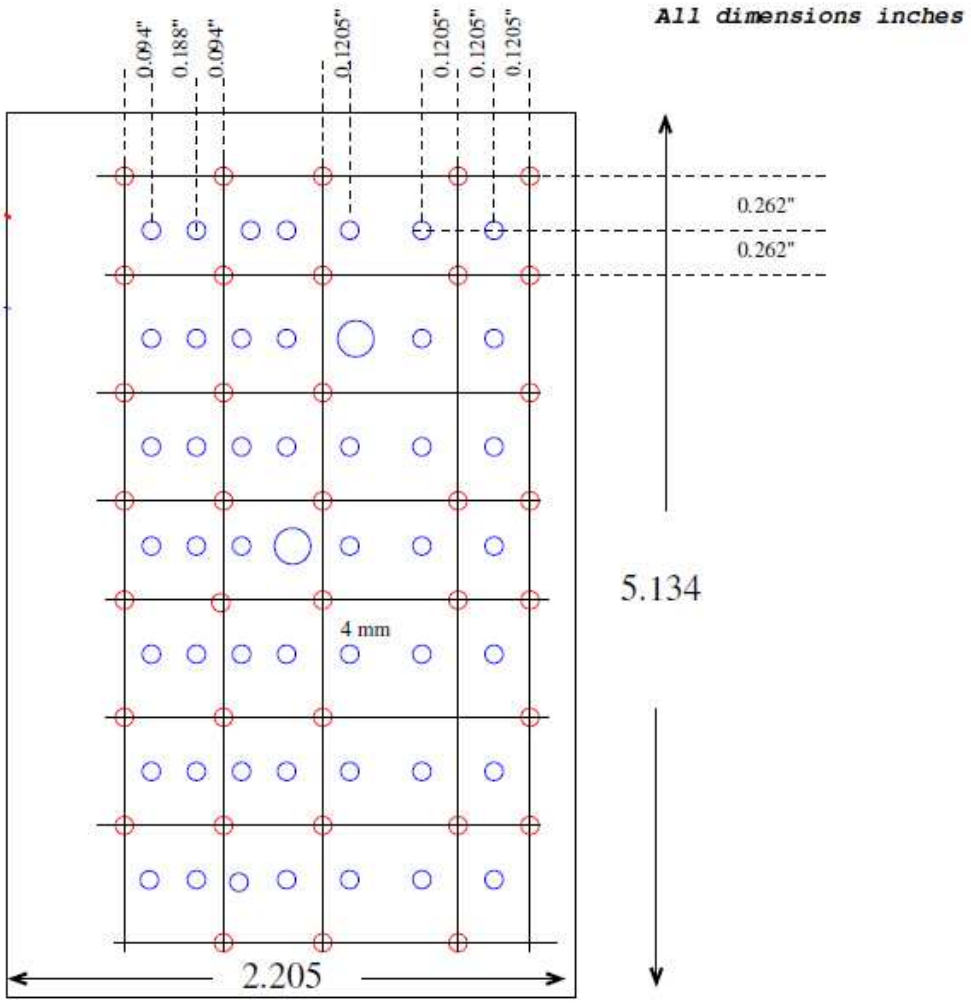

Figure 4: PREX sieve slit

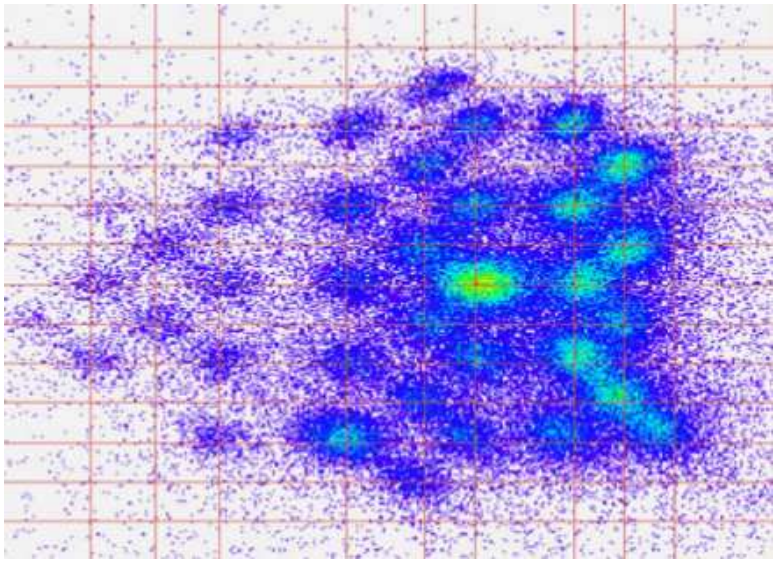

Figure 5: Optimized left θ_{tg} versus ϕ_{tg} sieve patterns

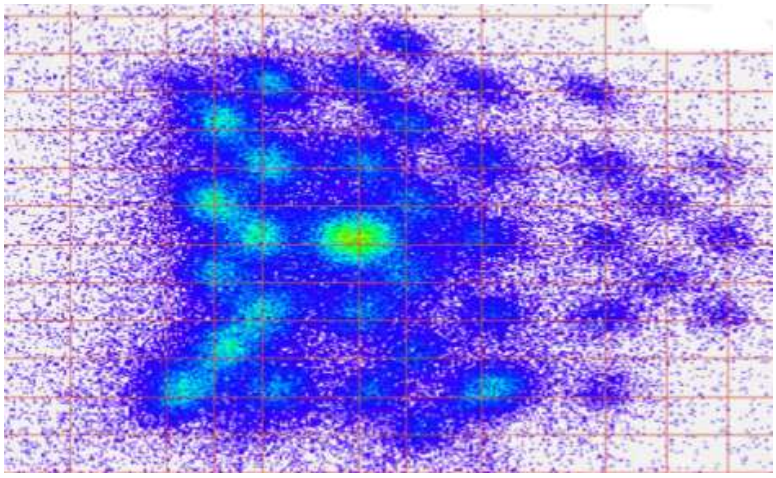

Figure 6: Optimized right θ_{tg} versus ϕ_{tg} sieve patterns

The cross points between vertical and horizontal lines are the expected location of sieve holes. By comparing the average locations with the expected values, one can find the errors from optics reconstruction.

Arm	σ_{θ_0} (°)	$\sigma_{\theta_{tg}}$ (°)	$\sigma_{\phi_{tg}}$ (°)
Left	0.020	0.066	0.017
Right	0.020	0.091	0.011

Table 7: Errors from all angle measurements

Combining all errors from θ_0, θ_{tg} and ϕ_{tg}, the average systematic error from scattering angle would be:

Arm	σ_θ (°)	σ_θ/θ (%)
Left	0.024	0.49
Right	0.021	0.43

Table 8: Errors of scattering angles

These errors in scattering angle measurement contributed $\sim 0.9\%$ to δQ^2.

2 Average Q^2 Analysis

PREX only selected events that passed through the four PREX detectors, two on each spectrometer. To ensure the correct hits, events were required to have nonzero ADC amplitudes after pedestal subtraction.

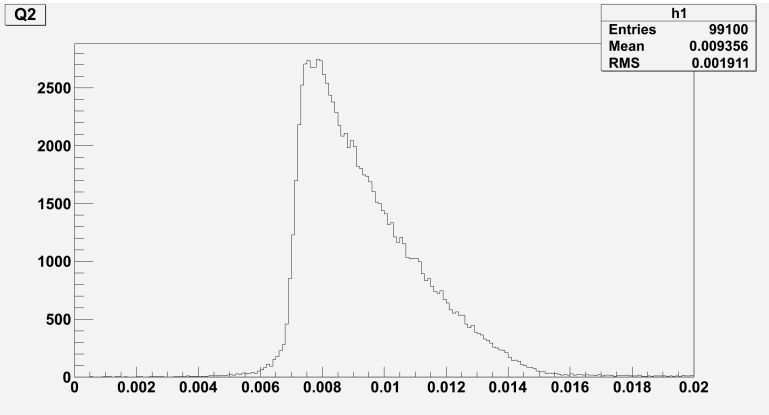

Figure 7: Q^2 distribution on LHRS

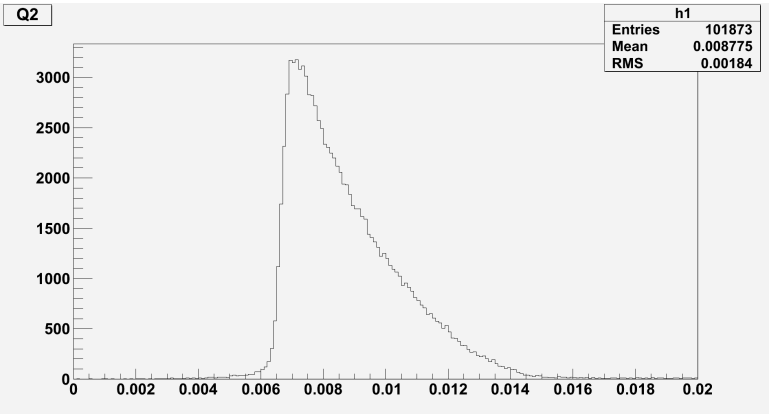

Figure 8: Q^2 distribution on RHRS

Fig. 7 and 8 show Q^2 distributions on both left and right spectrometers after applying ADC amplitude cut.

We also observed shifts in Q^2 as much as 1% between runs. These shifts could be explained by the shifts in average beam position for detected events. The shifts in averaged beam position can be due to two reasons:

1. After taking the beam for several days, some parts of target melted away and became nonuniform. This reduced the yeild for those thinner parts and, with the raster on, the average beam position seen by the detectors changed.

2. Due to the low beam currents, the beam position locks were not in place. This may have caused the actual beam position to change.

The change in beam position to one side would increase Q^2 on one spectrometer and decrease Q^2 on the other spectrometer. Since the beam position monitors did not operate during PREX due to low beam current, we had to determine the change in beam position by observing y_{tg} instead. Note that

$$z_{react} = -(y_{tg} + D)\frac{cos(\phi_{tg})}{sin(\theta_0 + \phi_{tg})} + x_{beam}cot(\theta_0 + \phi_{tg}) \tag{5}$$

where z_{react} and x_{beam} are the interaction position along the beam and horizontal beam position at the target respectively. For PREX, z_{react}=0.

The following figure illustrates how well y_{tg} were calibrated compared to known beam positions.

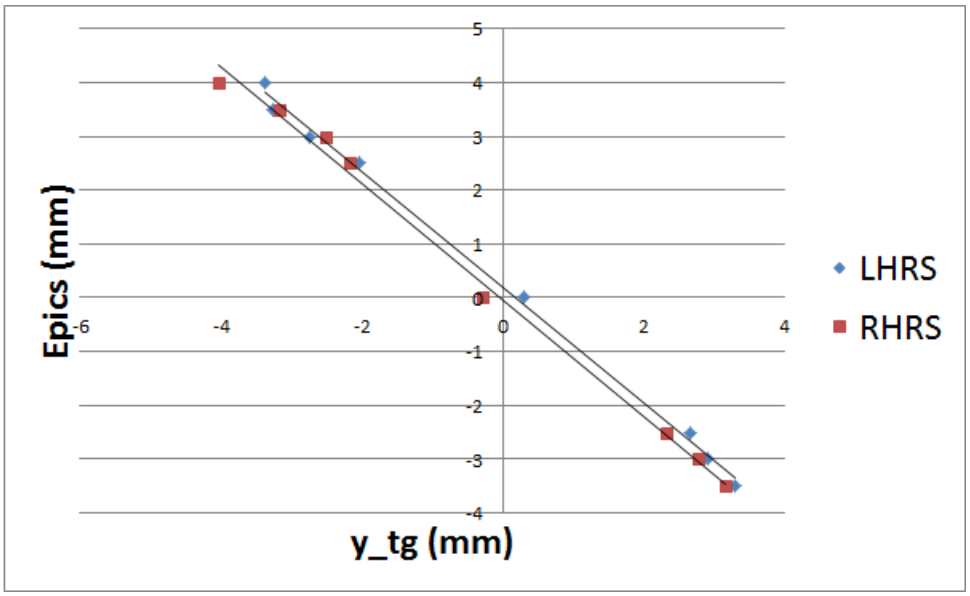

Figure 9: The relationship between calibrated y_{tg} and known beam positions

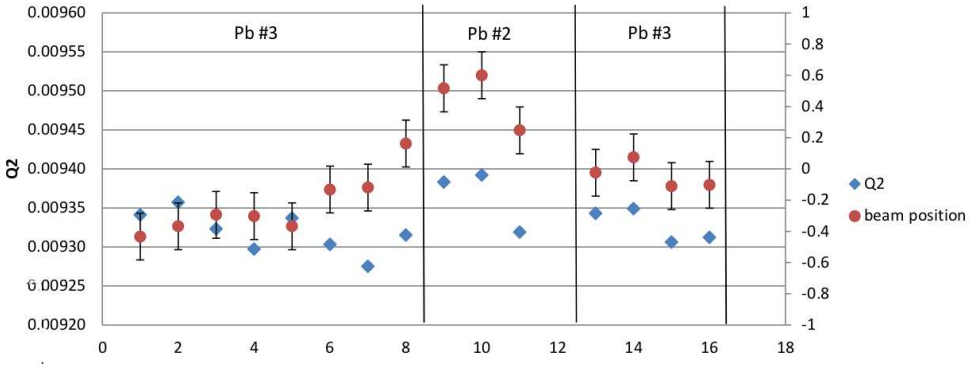

Figure 10: Q^2 distribution versus beam position on LHRS

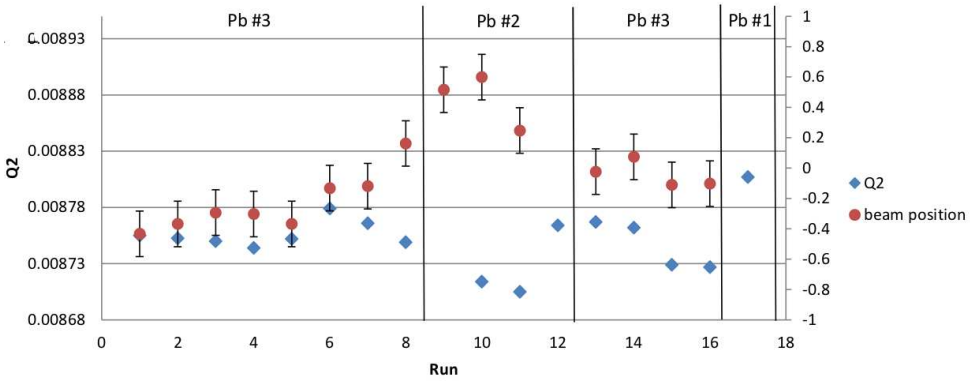

Figure 11: Q^2 distribution versus beam position on RHRS

As seen in fig. 10 and 11, once the average beam position moved to one side, Q^2 on one spectrometer increased while decreased on the other spectrometer.

3 Other systematic errors

3.1 Pileup

Pileup effects could occur from running at too high trigger rate which decreased the performance of vertical drift chamber (VDC). To determine this effect, we changed trigger rates from very low rate to extremely high rate and considered the VDC performance from Q^2 distribution.

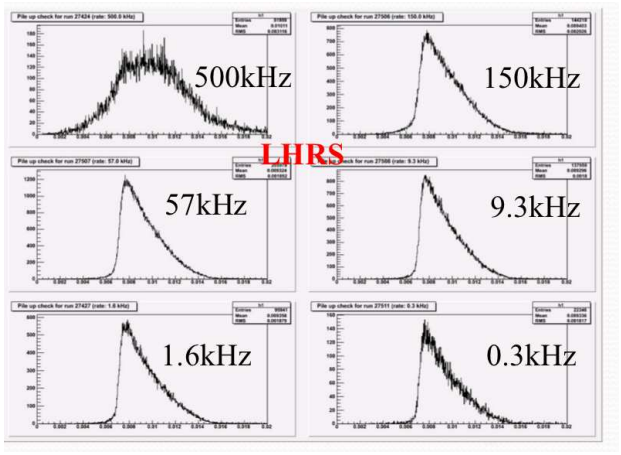

Figure 12: Q^2 showing VDC performance at different trigger rate (LHRS)

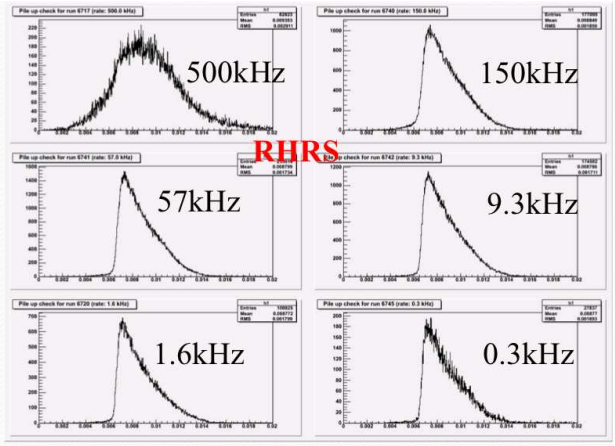

Figure 13: Q^2 showing VDC performance at different trigger rate (RHRS)

Clearly, pileup occurred when we ran at very high rate (500 kHz). Next figure shows how the average value of Q^2 depended on trigger rates.

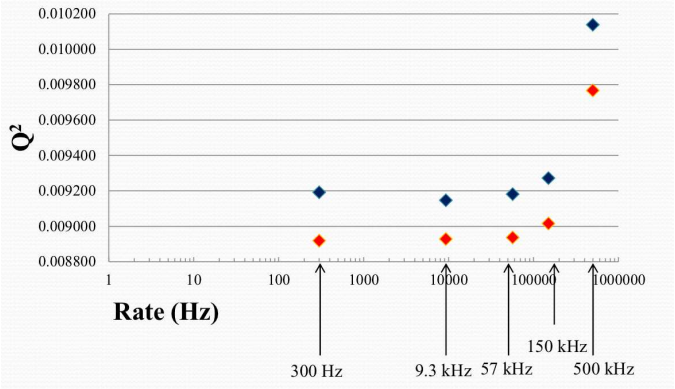

Figure 14: Q^2 dependence on trigger rate (higher values at the same rate are LHRS)

To reduce the effect of pileup, we only selected runs with the trigger rate lower than 100 kHz. However, even at lower trigger rate, pileup effects still occurred. The effect could be estimated by comparing Q^2 for different cuts on the number of tracks in the event. Using a 1-track cut versus allowing multiple tracks makes a shift of -0.06 $\pm$ 0.05% average shift on Q^2 We will take this variation in this as a systematic error.

3.2 Trigger Bias

PREX used two types of trigger: T1 and T5. T1 was the scintilator above the VDC planes while T5 was the main trigger used during the run and was placed above the PREX detector. By running T1 and T5 both seperately and simultaneously, T5 gave $Q^2 \sim 0.2$ % higher than T1. We will take this difference as a systematic error from trigger bias.

4 Results and conclusions

In summary:

1. PREX ran successfully and obtained enough information on Q^2 measurement.
2. Pointing measurement accurately determined spectrometer central angle (θ_0) with twice accuracy better than a survey.
3. An ADC amplitude cut on PREX detectors adequately ensured scattered particles hitting PREX detectors.
4. Trigger bias due to different types of trigger was small (0.2%).
5. Pileup due to VDC performance was small (<0.1%)
6. A 1% fluctuation in Q^2 was due to the change in average beam position.
7. Systematic errors for Q^2 was 1.0% as proposed.

Average LHRS Q^2 (GeV^2)	0.009330
Average RHRS Q^2 (GeV^2)	0.008751
Average Q^2 (GeV^2)	0.009066

Table 9: Q^2 summary for PREX

Table 9 shows the average Q^2 for both left and right spectrometer and also the average Q^2 of the experiment.

Error Source	Error (in source units)	Percent Error in Q^2
Beam Energy	1 MeV	0.1%
Final Momentum	1 MeV	0.1%
Scattering Angle	0.023°	0.9%
Pileup		<0.1%
Trigger Bias		0.2%
Total Systematic Error		0.1%
Statistical Error		<0.1%
Total Error		1.0%

Table 10: Summary of errors in Q^2 for PREX

Table 10 summarizes the errors which add in quadrature to 1.0% error. The largest error was from scattering angle measurement.